

# Identification of Acoustic Emission Sources as Important Factor in Study of Deformation's Stages of Loaded Materials

Oleg BASHKOV \*, Sergey PANIN \*\*, Tatiana BASHKOVA \*, Anton BYAKOV \*\*

\* Komsomolsk-on-Amur State Technical University, Komsomolsk-on-Amur, Russia

\*\* Institute of Strength Physics and Materials Science SB RAS, Tomsk, Russia

**Abstract.** Acoustic emission (AE) has been successfully used in non-destructive testing and materials research. Choice of the identification method of AE signals sources play an important role under reliable analysis of investigation results. Among the known methods of the AE source identification one can distinguish the techniques based on amplitude and energy distribution, b-value (energy-based methods) and methods based on analysis of AE signals frequency distribution (frequency-based methods). There are also combined methods for identification of AE sources.

The paper presents results of studies of the deformation behavior of metal-based alloys with the use of the AE method. The aim of this study was to establish the characteristic deformation stages as well as deformation mechanisms at each stage. Studies were carried out with the use of samples of low-carbon steels (0.2% and 0,45% C), aluminum alloys D16AT, AMg6AM (referred to in western literature as 7075, 5056), titanium alloys Ti-4Al, Ti-6Al-2Mo-2Zr. The method of identification of AE sources is offered based on the analysis of two-parameter distribution (frequency parameter Kf vs energy of AE signals E). The frequency parameter Kf is based on wavelet transform of AE signals. The method offered has allowed locating at the two-parameter distribution (E-Kf) of AE signals emitted under plastic deformation (with characteristic AE sources like dislocations, twins) and fracture (micro-and macro-cracks) of materials.

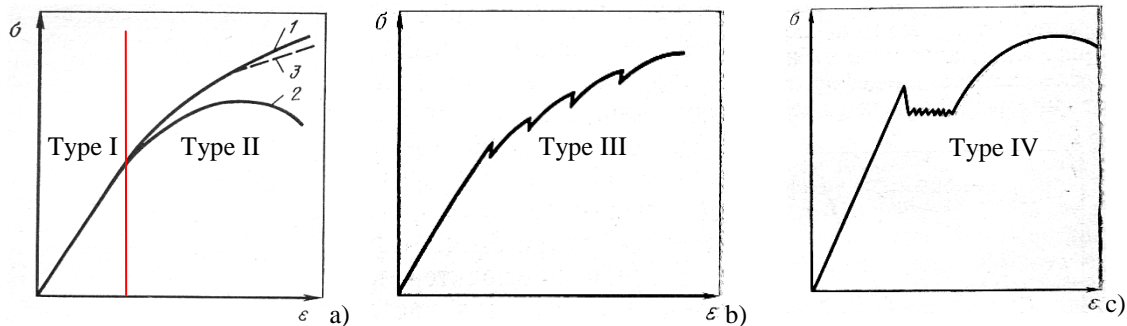
The investigation results have allowed establishing the presence of various types of AE signals at various stages deformation. With the use of AE method there was confirmed manifestation of the Portevin – Le Chatelier dislocation mechanism effect at discontinuous yielding in AMg6AM alloy (5056 Al alloy). By the analysis of AE emission signals it is shown the dislocation type mechanism of dispersion hardening in aluminum alloy D16AT (7075 Al alloy). The paper presents result that that characterize the influence of loading rate and structural state (composition) on the AE parameters. With the change the loading rate the AE activity and AE count of various AE sources (dislocations, microcracks) is changed but in different manner and not monotonically.

## Introduction

Deformation of the material is a complex multi-level multi-stages process involving different mechanisms of plastic deformation and fracture. Formed defect structure determines patterns of future behavior of the material during deformation. R. Herzberg was the systematization of data about the kinds of stress-strain curves for materials with



different types of crystal lattice and the structural state [1]. Identified four types of deformation characteristic of metals and alloys. Type I - elastic behavior characteristic of all types of materials at the initial stage of reversible deformation obeys Hooke's law (pic. 1, a). Type II – elastic homogeneous-plastic behavior of materials capable of irreversible plastic deformation for materials with fcc and hcp lattice (pic. 1, a). Type III – elastic heterogeneous-plastic behavior of materials with a characteristic has an effect of unstable plastic flow and bears the name of the effect Portevin - Le Chatelier (pic. 1, b). He described for dilute solid solutions of aluminum [2-4]. Type IV is defined as deformation elastic heterogeneous-plastic homogeneous-plastic behavior (pic. 1, c) with the development of the local Luders slip bands.



**Pic. 1.** Behaviors stress-strain curve. 1 - true strain curve, 2 - curve relative deformations, 3 - curve corrected values

Deformation of the material occurs with the change of stages. Each stage is characterized by a set of mechanisms and their contribution to the overall process of deformation.

Explanation of material behavior is challenging enough. Fact that the behavior of a deformable material is influenced by all elements of the structure together and each element separately. Acoustic emission (AE) during the deformation and fracture of materials contains a wealth of important information about the physical processes, changes in the structure of the material, fracture energy, strain rate, etc. In the literature there are studies which have analyzed not only the aggregate AE signals during the test materials, but also the analysis of individual AE signals for the purpose of detailed transcripts and identification. However, the complexity of the parametric description of the propagation of acoustic waves in a limited, non-defective, an anisotropic medium is not yet possible to develop a unified theory of signals and identification of AE sources. Previously in the literature were presented work on the use of frequency analysis [5-7] and wavelet analysis [8] to assess the nature of AE signals. New results studies of the relationship of AE signals with the mechanisms of structural changes in materials can be one of the important research practical problems of modern materials.

In the present paper analyzes the features of deformation and fracture of some constructional materials with different types of deformation behavior using the AE method to identify the types of AE sources and corresponding mechanisms of deformation and fracture.

## 1. Materials and experimental method

Studies were carried out on the structural materials with different types of deformation. In certain modes of deformation in the annealed condition and low-carbon steels pure iron can manifest Luders deformation with characteristic tooth strength. For this experiment mild steel was used in the normalized condition 20 with a carbon content of 0.2%. 20 steel is

widely used in engineering and manufacturing of power equipment. Strain diagram steel platform 20 has strength without significant yield tooth.

Of the elastic-plastic behavior of homogeneously conducted on aluminum alloy D16AT (referred to in western literature as 7075) in the state quenching and aging. Manifestation of the effect of intermittent flow Portevin–Le Chatelier examined for aluminum alloy AMg6AM (referred to in western literature as 5056) in soft annealed condition delivery.

Tensile tests were performed at the strain rate  $2 \cdot 10^{-4} \text{ s}^{-1}$  on the test machine INSTRON-5582. Samples of sheet materials were made of 2 mm thick. Samples of steels were produced by laser cutting, and aluminum and titanium alloys contour milling. Cross-section samples in the test section was  $2 \text{ mm} \times 2 \text{ mm}$ . When analyzing the results were used graphics voltage  $\sigma = f(\epsilon)$  and strain hardening  $d\sigma/d\epsilon = f(\epsilon)$ , obtained by the "machine" diagram load testing machine. This approach proved to be the most successful to align in time and strain loading schedules and acoustic emission. Separation stage was the diagram of strain hardening as the most studied in terms of the analysis of deformation processes at the macro level. Using this approach, the diagram  $d\sigma/d\epsilon = f(\epsilon)$  highlighted a number of major steps.

Registration of AE signals was performed on laboratory complex with integrated four-channel high-speed ADC on a sampling frequency of 10 MHz. Amplifier gain 55 dB in the frequency band 30 - 800 kHz. For registration of AE signals were used AE broadband transducers GT301 firm GlobalTest with bandwidth 50 - 500 kHz.

Transducers installed at the edges of the sample: one on each side. Analysis of the mechanisms of destruction of materials was carried out on the parameters obtained on the basis of spectral analysis and wavelet analysis of AE signals [9, 10], as well as traditionally used parameters - energy AE signals. Registration was performed using signals of two channels to determine AE source location.

To decrypt the signals and identification of AE sources was used wavelet analysis of AE signals. Earlier findings suggest that the formation of AE signal is influenced by such parameters as the rate of deformation source and the increment of deformation. The increment of deformation and deformation rate is indirectly related to the frequency and energy of the acoustic elastic wave occurs during deformation. Thus, the energy of the excited wave depends on the speed of micro-defects. According to [5], the slip occurs in local regions with speed up to 500 m/s, while the rate of formation of voids (microcracks) is about 1500 m/s. Frequency can be implicitly defined as  $f \approx \frac{V^2}{c_{l,t} \cdot L}$ , where  $V$ -speed

moving of defects,  $L$  - their characteristic size,  $c_{l,t}$  - the group velocity of sound in the material [11].

We can conclude that one of the main criteria for determining the type of power source deformation and AE are the energy and frequency of the acoustic radiation. Emission spectrum of AE signals is quite wide. Using Fourier spectrum analysis of AE signals is not quite correct, because truthfully describes a harmonic signals. However, AE signals are stochastic. Therefore, the use of Fourier analysis to assess the frequency of AE signals is not always justified. In this regard, the frequency of the wavelet analysis can yield additional information about the complex processes of deformation. Registered in the deformation process AE signals were analyzed using Daubechies wavelet decomposition of order 8 with a central frequency of 0.667, which allowed to cover the entire spectrum of the signals useful. On the basis of wavelet coefficients detailing identification was calculated parameter called frequency coefficient  $K_f$ , determines the magnitude of the contribution of individual frequency components of the signal spectrum in AE as a whole. Frequency factor  $K_f$  was calculated by formulas (1, 2):

$$stdFQ_j = \sqrt{\frac{1}{n} \sum_{i=1}^n (x_{ji} - \bar{x}_j)^2},$$

$$K_f = \sum_{j=1}^m (stdFQ_j \cdot (m+1-j)) / \sum_{j=1}^m (stdFQ_j),$$

where  $stdFQ_j$  - the standard deviation of the  $j$ -th wavelet coefficients of AE signal,  $n$  - the number of discrete samplings of AE signal,  $m$  - the number of wavelet coefficients,  $x_{ji}$  - numerical value of the  $i$ -th discrete samplings of the  $j$ -th wavelet coefficient,  $\bar{x}_j$  - average number of the  $j$ -th wavelet coefficient.

The physical meaning of the frequency coefficient  $K_f$  is defined as the contribution to the spectrum frequency components in the whole signal AE. The energy component of each frequency component is defined with respect to the time of its excitation (taken into account the phase shift of the frequency components of the wavelet analysis technology). Value of the frequency coefficient  $K_f$  is greater, the more energy contribution to the acoustic signal frequency components and a smaller phase difference between frequency components.

### 3. Results of experimental studies

On the basis of [1] were selected three typical types of dependencies  $\sigma = f(\varepsilon)$  with different behavior curve  $\sigma - \varepsilon$  on pic. 1, which were built according to  $d\sigma/d\varepsilon = f(\varepsilon)$ :

- elastic homogeneously-plastic behavior with hardening without a yield plateau (type *I* and *II*),
- elastic heterogeneously-plastic behavior with the presence of unstable plastic flow (type *III*),
- elastic homogeneously-plastic behavior with a yield plateau and the subsequent strain hardening (type *IV*).

According to the results of tests of alloys samples D16AT, AMg6 and steel 20, based on diagrams  $\sigma = f(\varepsilon)$  were built hardening function  $d\sigma/d\varepsilon = f(\varepsilon)$  (Fig. 2). When analyzing the results were used graphics stress  $\sigma = f(\varepsilon)$  and strain hardening  $d\sigma/d\varepsilon = f(\varepsilon)$ , obtained by the "machine" diagram load testing machine. This approach proved to be the most successful to align in time and strain graphs stress and AE. Separation stage was the diagram of strain hardening  $d\sigma/d\varepsilon = f(\varepsilon)$ , as the most studied in terms of the analysis of deformation processes at the macro level. Technique for separation stages was based on identifying areas depending  $d\sigma/d\varepsilon = f(\varepsilon)$  with a stationary steady process. Identified five major and several intermediate stages of stationary steady-state deformation:

I - elastic stage (depending on the elastic properties of the test material portion of the curve  $d\sigma/d\varepsilon = f(\varepsilon)$  may take the form of horizontal section corresponding to a constant ratio  $d\sigma/d\varepsilon$ , or take the form of an increasing function);

II-plastic deformation Luders (characterized by a significant decrease in  $\varepsilon d / \sigma d$  high steepness graphics). For strain type IV - stage is divided into two intermediate stages: II<sub>1</sub> - beginning of plastic flow, II<sub>2</sub> - easy gliding (characterized by horizontal section dependence  $d\sigma/d\varepsilon \sim 0$ ;

III - stage of strain hardening. For strain type II and III - stage with decreasing dependence on low speed  $d\sigma/d\varepsilon = f(\varepsilon)$ . For strain type IV - stage is divided into two intermediate stages: III<sub>1</sub> - transitional stage of growth depending  $d\sigma/d\varepsilon = f(\varepsilon)$  after the stage of easy slip, III<sub>2</sub> - stage with linear hardening  $d\sigma/d\varepsilon = \text{const}$ , III<sub>3</sub> - stage with a decreasing dependence on low speed  $d\sigma/d\varepsilon = f(\varepsilon)$ ;

IV - stage of localized deformation (characterized by a reduction graph of  $\sigma = f(\varepsilon)$ , associated with the localization of deformation). For the deformation type II and IV is linked to the localization of the neck formation in the region of future fracture. For strain type III - localization occurs abruptly at the time of unstable plastic flow in the bands of localized deformation (effect Portevin - Le Chatelier).

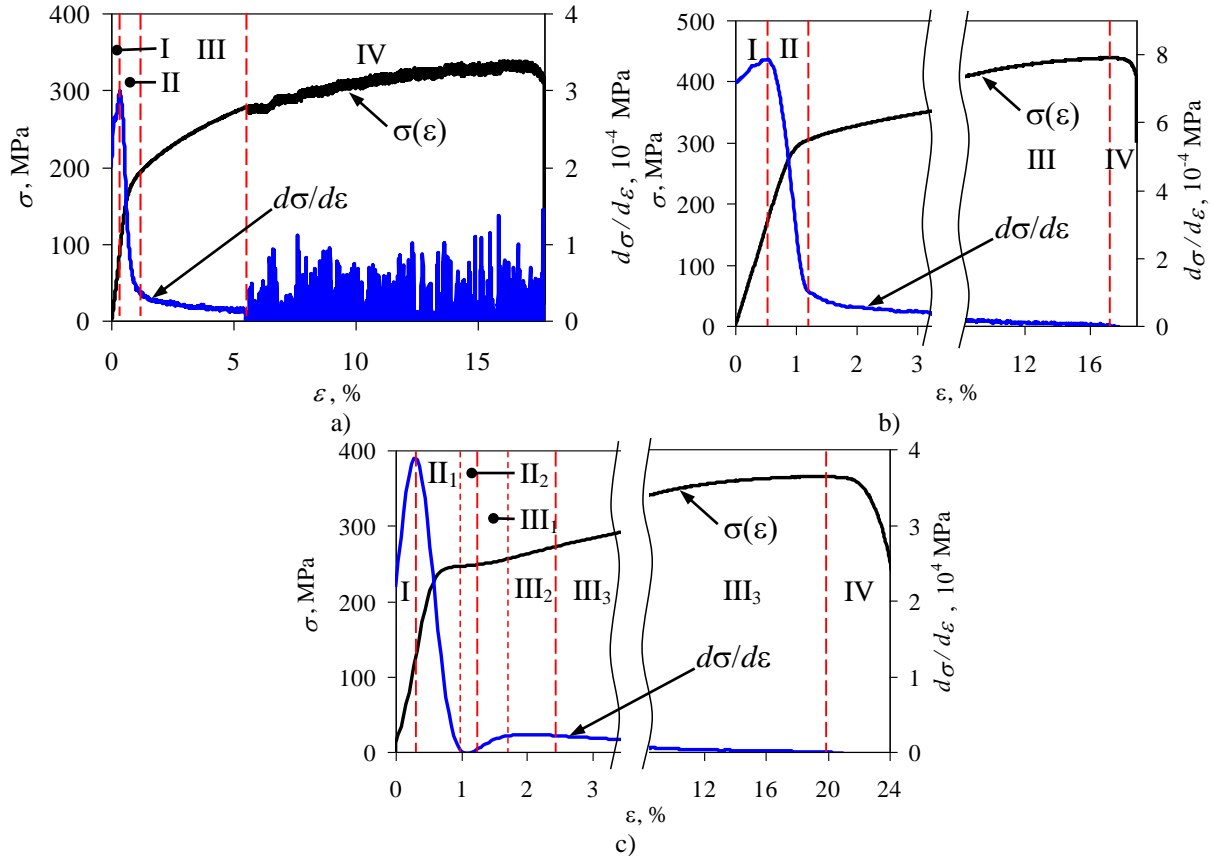


**Fig. 2.** Stress-strain  $\sigma(\varepsilon)$  and strain hardening  $d\sigma/d\varepsilon$  diagrams of samples: a) D16AT, b) AMg6AM, c) steel 20.

Next analysis consisted in the division of AE signals recorded during the test samples emitted by different types of AE sources: dislocations, micro- and macro-cracks. Separation was carried out by the method of frequency-energy analysis of the previously approved on materials with homogeneous and inhomogeneous structure and heterogeneous materials with hardening coatings [10]. Field two-parameter distribution E-Kf (energy - frequency factor) of AE signals is divided into regions corresponding to the previously identified parameters of signals of different types of AE sources: dislocations correspond to the values of  $E < 0,8 \text{ mV}^2 \cdot \text{s}$  and  $K_f > 3,5$ ; microcracks –  $E = 0,8-20 \text{ mV}^2 \cdot \text{s}$  with  $K_f > 3,5$  and  $E < 20 \text{ mV}^2 \cdot \text{s}$  with  $K_f < 3,5$ ; macrocracks –  $E > 20 \text{ mV}^2 \cdot \text{s}$ . Diagrams of the two-parameter distribution E-Kf AE signals for the tested samples are shown in pic. 3.

Method for detecting areas is presented in [9, 10]. The procedure involved conducting multiple studies of plastic and solid materials in the same test conditions. During testing, the plastic deformation and recorded cracking of various sizes. Division of AE signals at the micro- and macro-cracks were suspended. Microcracks was assumed crack opening  $< 1-2 \text{ um}$ , macrocracks  $> 5-10 \text{ microns}$ . Signal parameters depend on the parameters of the equipment (converters, amplifiers) and sample sizes. Therefore, a comparative analysis without adjusting the parameters is possible only for some test conditions.

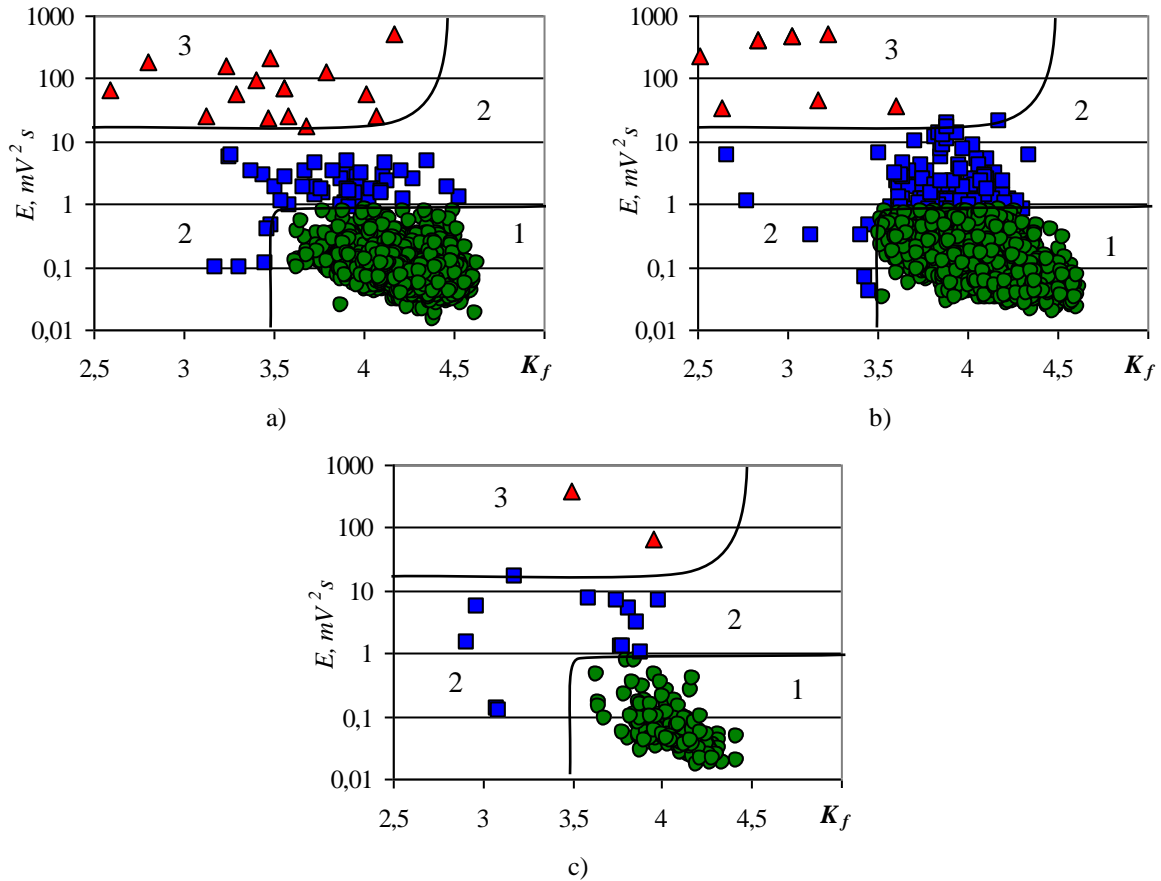


**Fig. 3.** Two-parameter distribution of E- $K_f$  AE signals recorded during the test samples: a) D16AT, b) AMg6AM, c) steel 20.  
(area: 1 – dislocations, 2 – microcracks, 3 - macrocracks)

The main purpose of the separation of AE signals by source types is to identify the deformation mechanisms at different stages of deformation. Fig. 4 illustrates the activity of AE signals  $dN/dt$ , separated by source types that are associated with the deformation curve  $\sigma(\varepsilon)$ . Marked on the charts stage allocated on the basis of dependence  $d\sigma/d\varepsilon = f(\varepsilon)$  from pic. 2. For each stage of the nature of the activity of AE signals of different types of sources identified general patterns and individual peculiarities of manifestation of deformation.

Stage I ( $\varepsilon = 0-0.5\%$ ) is classified as a stage on the basis of increasing elasticity values  $d\sigma/d\varepsilon$  for stage. By the end of stage I for all materials is observed if the first peak activity of AE. The first peak in step mikrotekuchesti AE can be associated with the collective movement and multiplication of dislocation in the grain boundaries of the surface layer is preferably, as well as their exit to the surface. Limbo new dislocations occurs mainly at grain boundaries and microconcentrator stresses directly on the metal surface. High speed stress increment  $d\sigma/d\varepsilon$  also causes the formation of microcracks at the grain boundaries, which is accompanied by increased activity of the corresponding AE sources  $dN/dt_{mic}$ . Most active dislocation type AE signals observed in the alloy AMg6AM:  $dN/dt_{disl} = 110 \text{ s}^{-1}$ .

Stage II ( $\varepsilon \sim 0.5-1.5\%$ ) – stage of plastic deformation. Stage is characterized by a high rate of descent  $d\sigma/d\varepsilon$  and declining activity in all types of AE sources for materials deformed by type II and III (pic. 1). For materials with a yield plateau stage II can be conditionally divided into two intermediate stages: II<sub>1</sub> - the beginning of plastic deformation and II<sub>2</sub> - point or stage of easy slip ( $d\sigma/d\varepsilon \sim 0$ ), which becomes noticeable only when a significant increase in scale  $\varepsilon$ .

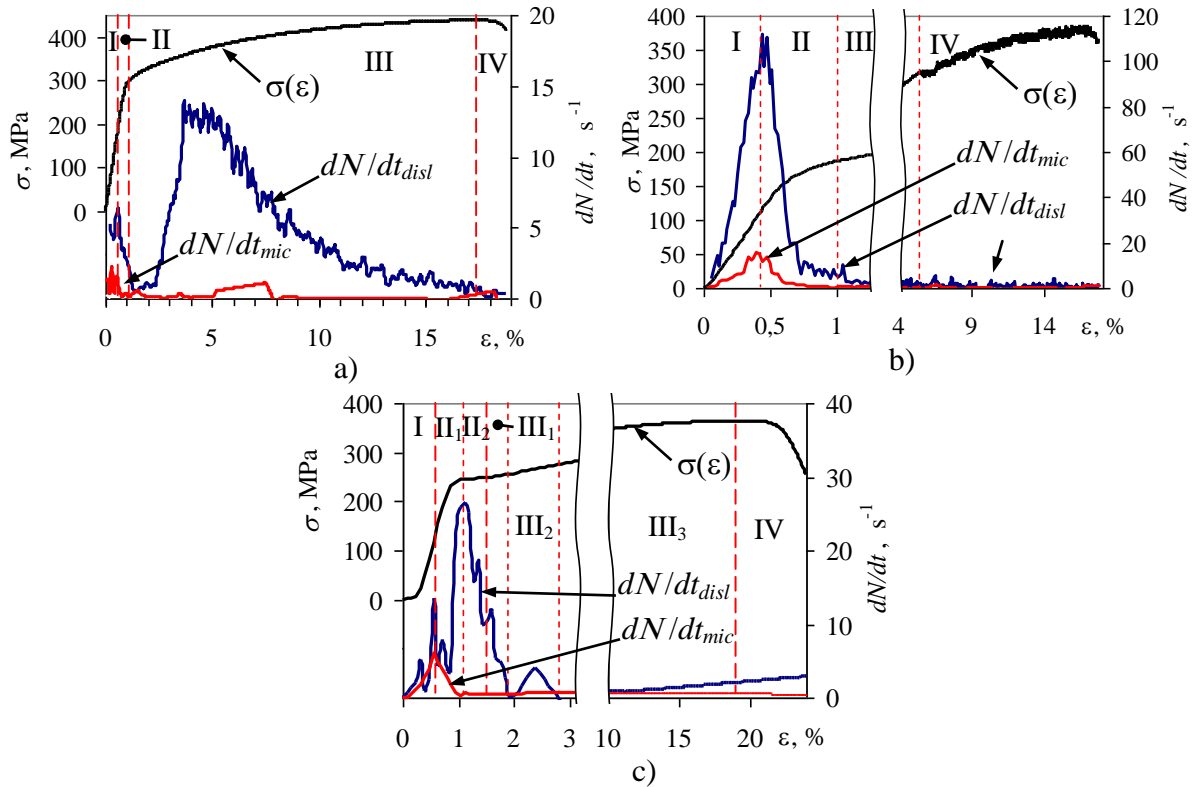


**Fig. 4.** Graphs of activity  $dN/dt$  of different types of AE sources: a) D16AT, b) AMg6AM, c) steel 20

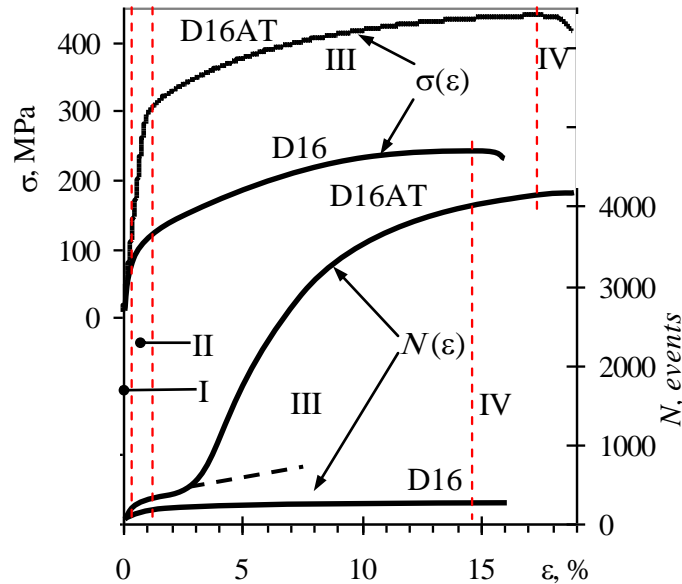
For materials with a yield plateau, deforming type IV (Fig. 1), characterized by the presence of the second peak activity of AE signals dislocation type  $dN/dt_{disl}$  stage II<sub>2</sub> (pic. 4, c). The second peak of activity AE usually higher than the first, as is typical for most low-alloy and carbon steels with strain type II (pic. 1). AE activity peaks during the passage of the Luders strain on the yield plateau associated with avalanche breakthrough dislocations throughout the volume of the metal on the front line strength. The main factors are also processes dislocations to the surface and increase the density of dislocations at the grain boundaries.

Stage III work hardening is the most extensive and interesting features in relation to structural changes in various materials. A feature of this stage is to reduce the general level of activity of AE. At this stage, a significant increase in dislocation density in a yield of dislocation clusters at grain boundaries and phase boundaries inclusions and the formation of a cellular dislocation structure with a dislocation density and the critical submicrocracks formation [12-14].

Increase in dislocation density leads to a reduction in the mean free path and the density of mobile dislocations (reduced amplitude and energy of AE signals). Intermediate stage of linear hardening steel 20 III<sub>2</sub> characterized by a small increase in the activity of dislocation type AE signals at this stage. Few signals are registered as microcracks. Decrease of coefficient  $d\sigma/d\varepsilon$  at the intermediate stage III<sub>3</sub>, the final strain hardening steel 20 flows with low AE activity.

Another mechanism is registered in step strain hardening alloy D16AT. Low level of AE activity by the end of stage II is replaced by the growth of dislocation type AE activity when the strain  $\varepsilon \sim 3\%$  for stage III. Peak activity  $dN/dt_{disl} = 15 \text{ s}^{-1}$  is achieved when  $\varepsilon \sim 5\%$ . Explanation of this phenomenon lies in the mechanism of strain hardening alloy D16. It is known that copper-containing aluminum alloys are strengthened by dispersion hardening mechanism. On the particles formed during the aging of the second phase is formed during deformation of dislocation loops with a consequent increase in the density of dislocations and hardening.

Generation of dislocations caused by the formation of dislocation loops, leads to significant acoustic emission, highlighting, so at the micro stage precipitation hardening was not observed at the macro and meso levels. Radiated with AE signals have little variation of parameters  $E = 0,04-0,4 \text{ mV}\cdot\text{s}^2$ ,  $K_f = 4,0-4,5$ . In support of this study, results were obtained deformation annealed alloy D16, obtained by annealing the samples D16AT at  $t = 440^\circ \text{C}$  (pic. 5).



**Pic. 5.** Graph  $\sigma=f(\varepsilon)$  and  $N=f(\varepsilon)$  for the alloy samples of samples D16AT and D16

After annealing, the tensile strength is reduced from 440 to 215 MPa, the ductility decreases slightly to 16%. AE count in the first two stages of qualitatively the same form depending  $N(\varepsilon)$  for tempered and hardened D16AT (pic. 4, a). AE count at the beginning of stage III for the annealed sample D16 is considerably smaller than the quenched and aged sample D16AT. Signals from microcracks on the sample stage III D16 virtually absent in contrast to D16AT. AE activity for sample D16 significantly reduced until fracture.

AE activity during the deformation of the sample alloy AMg6AM stage III low but rather constant  $dN/dt_{disl} = 2-4 \text{ s}^{-1}$ . In some moments recorded AE signals from microcracks. AE activity is maintained until the beginning stages of intermittent flow.

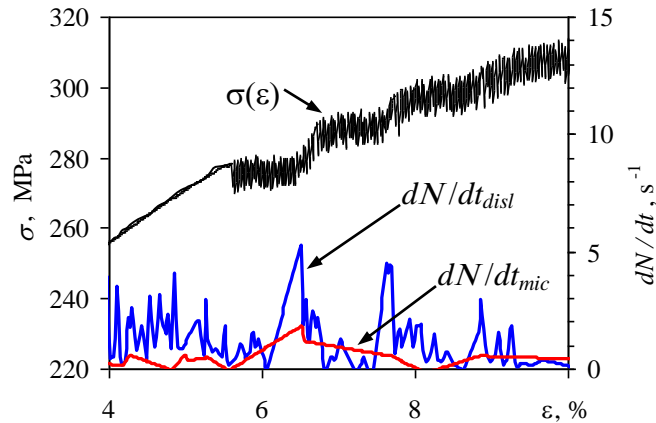
The final stage IV characterized by localization of deformation. However, the mechanisms of its manifestations are different for different materials. Macrolocalization deformation, accompanied by formation of a neck, usually leads to a significant reduction in the activity of AE until complete disappearance. Such observed for materials deformed by type II and IV. These include alloy D16AT and steel 20. This is due to a decrease in the deformed volume, increasing the density of dislocations and significant grain refinement in the localized volume. Last often results in the appearance of the grain boundary plasticity, having a low level of energy emitted by the AE signals. AE activity can only occur before the destruction.

Nevertheless, intermittent flow is defined as the instability of local plastic deformation not resulting in total loss of stability.

Appearing on the alloy AMg6AM effect of unstable plastic flow is also a manifestation of strain localization, the nature of which is not yet fully understood. Intermittent flow is a manifestation of the inhomogeneity of plastic deformation at the meso level. Necking is considered a manifestation of the inhomogeneity of plastic deformation at the macro level. The transition from one to the other meso level and the transition from meso to macro level is quite conventional. Although the macro-level is considered to be at the level of the whole object and the deformation at the macro level described by the

diagram depending  $\sigma(\varepsilon)$ . Nevertheless, intermittent flow is defined as the instability of local plastic deformation not resulting in total loss of stability. Therefore, intermittent flow can be attributed to stage IV, characterized as a stage of strain localization.

When installed strain rate  $\dot{\varepsilon} = 2 \cdot 10^{-4} \text{ s}^{-1}$  regular relaxation oscillations with voltage deviation  $\Delta\sigma \sim 8\text{-}12 \text{ MPa}$  and periodicity  $T \sim 1 \text{ s}$  already starts when the strain  $\varepsilon = 5,5 \%$  (pic. 6).



**Pic. 6.** Fragment of stress-strain diagram  $\sigma(\varepsilon)$  of samples AMg6AM and AE activity  $dN/dt$  graphs

Effect of unstable plastic flow occurs in a periodic pattern of localized slip material. After about 30 periodic surges average voltage level rises within  $\varepsilon \sim 0,4 \%$ , forming a transition to the next level of deforming stress and a kind of "shelf" mid-level voltage deviation. Duration formed on the graph deformation curve "shelves" equals  $1,0\%$ , which corresponds to the deformation time  $\sim 30$ . After the transition to the next higher level of the average value of voltage deviation voltage increases to  $\Delta\sigma \sim 12 \text{ MPa}$ . Wherein AE is small enough and the activity is recorded for signal  $\leq 1$  second. In the transition to the next level of higher voltages, there is increased activity of AE signals dislocation type to  $dN/dt = 6 \text{ s}^{-1}$  (pic. 6).

## Conclusions

Based on the studies, the following conclusions:

- Effective description of deformation mechanisms using acoustic emission method is made possible by separating signals and identification of AE sources/
- Step strain, isolated on the basis of function of work hardening  $d\sigma/d\varepsilon = f(\varepsilon)$ , consistent with the AE activity for different types of AE sources in these stages.
- Stages of elasticity (mikrotekuchesti) and plastic deformation Luders for various materials have common parameters AE and characterized by one or two peaks of activity AE. AE parameters in step strain hardening significantly depend on the characteristics of the heterogeneous structure of deformable materials. Identify common parameters AE stage IV shows the possibility of classifying stage unstable plastic flow and macrolocalization to the manifestation of strain localization at different scale levels.

## References

- [1] R. Hertzberg, Deformation and fracture mechanics of structural materials. Lane. from English. Ed. ML Bernstein, SP Efimenko. Moscow: Metallurgy. 1989. 576 p.

- [2] AH Cottrell: Vacancies and Other Point Defects in Metals and Alloys, pp.1-40, Inst. of Met., London, 1958.
- [3] YI Golovin, Ivolgin VI, Region of existence of the effect Portevin - Le Chatelier in continuous indentation alloy Al-2.7% Mg at room temperature // Solid State Physics. - 2004. - T. 46. - Vol. 9. - pp. 1618-1620.
- [4] Bell, JF Experimental foundations of mechanics of deformable solids. Nauka. - 1984. - Part 2. - 431 p.
- [5] Muravin GB, Simkin YV, AI Merman, Identifying the mechanism of destruction of materials methods of spectral analysis of acoustic emission signals // Defectosopia. - 1989. - № 4. - pp. 9-15.
- [6] AP Braginsky, Defect detection by the spectral characteristics of acoustic emission // Defectosopia. - 1984. - № 1. - S. 47-55.
- [7] A. Bragin, BM Medvedev, AI Platkov, Amplitude-frequency technique locations acoustic emission sources // Defectosopia. - 1988. - № 8. - pp. 58-65.
- [8] Hamstad MA, Gallagher AO and Gary J. Examination of the Application of a Wavelet Transform to Acoustic Emission Signals: Part 1. Source Identification // J. Acoustic Emission. - 2002. - V. 20. - P. 39-61.
- [9] Bashkov OV, SV Panin, Semashko NA, Petrov VV, Shpak DA, Identification of sources of acoustic emission during deformation and fracture of steel 12X18H10T // Zavodskaja laboratorija. Diagnostika materialov. - 2009. - № 10. - pp. 51 - 57.
- [10] Bashkov OV, SV Panin, AV Byakov, Investigation of influence of the thickness of the nitrated surface layer on the staging of the deformation and fracture of steel 12X18H10T acoustic emission method, correlation analysis of digital images and diagrams of loading // Physical Mesomechanics. - 2010. - № 6. - T. 13. - S. 53-72.
- [11] VA Krasil'nikov, VV Krylov, Introduction to physical acoustics. - Moscow: Nauka. - 1984. - 403.
- [12] J. Radon, Dependence of crack growth rate in fatigue under cyclic loading with constant amplitude // Physical Mesomechanics. - 2000. - V.3. - № 2. - Pp. 81 - 89.
- [13] AG Penquin Terent'ev VF Assessment of the degree of damage to structural steel 19G for statistical and cyclic deformation using acoustic emission // Metals. -2004. - № 3. - pp. 78-85.